



**Politecnico
di Torino**

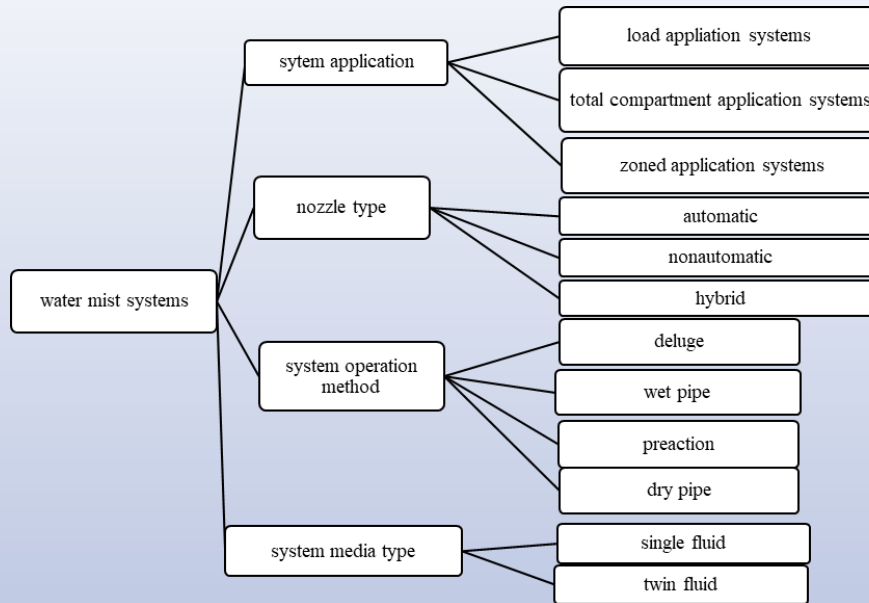


IWMA
International Water Mist Association

CFD Modeling of Water Mist Systems for Suppressing Shielded fires in Enclosures Using FDS

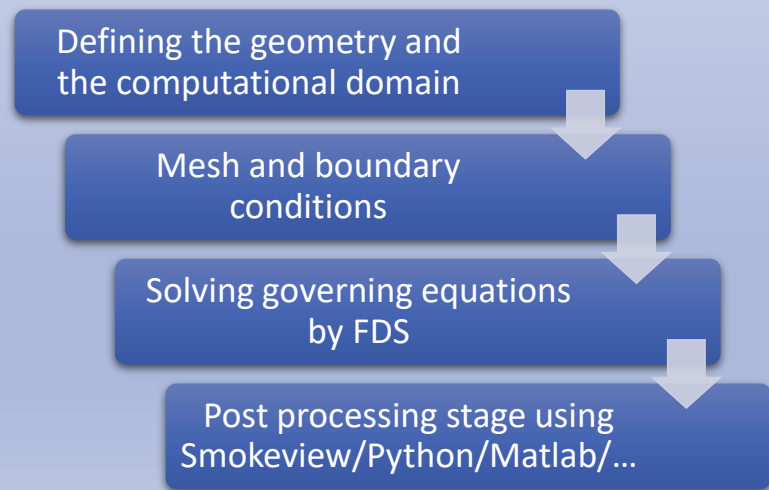
Speaker:
Azad Hamzhepour
Department of Energy
Politecnico di Torino, Italy

- Introduction
- Methodology
- Results
- Conclusions



NFPA 750

Type	Range of pressure (bar)
Low-pressure	≤ 12.1
intermediate	> 12.1 < 34.5
High-pressure	≥ 34.5



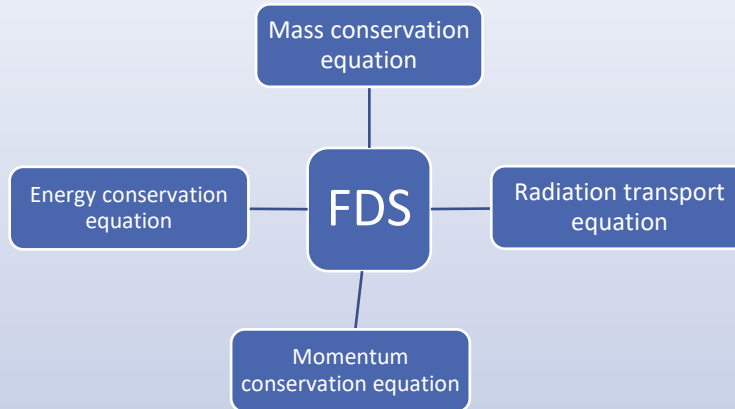
- **The use of water mist systems in tunnels, residential and commercial buildings, garage, parking lots, etc.**
- **Designing the proper water-based fire suppression system and proper positioning**
- **Validation and verification of the designed numerical model with available experimental or theoretical data**

Introduction

Methodology

Results

Conclusions



- State equation
- Initial and boundary conditions
- Turbulence models
- Pressure solver

$$\partial_t(\rho Z_\alpha) + \nabla \cdot (\rho Z_\alpha \vec{v}) = \nabla \cdot (\rho D_\alpha \nabla Z_\alpha) + \dot{m}_\alpha''' + \dot{m}_{b,\alpha}'''$$

$$\partial_t(\rho \vec{v}) + \nabla \cdot (\rho \vec{v} \vec{v}) = -\nabla p + \rho \vec{g} + \vec{f}_b + \nabla \cdot \tau_{ij}$$

$$\partial_t(\rho h_s) + \nabla \cdot (\rho h_s \vec{v}) = \frac{D\bar{p}}{Dt} + \dot{q}''' + \nabla \cdot \vec{q}''$$

$$\begin{aligned} & \frac{1}{c} \frac{\partial I_\lambda(x, s, t)}{\partial t} + s \cdot \nabla I_\lambda(x, s) \\ & = -\kappa(x, \lambda) I_\lambda(x, s) - \sigma_s(x, \lambda) I_\lambda(x, s) + B(x, \lambda) \\ & + \frac{\sigma_s(x, \lambda)}{4\pi} \int_{4\pi} \varphi(s', s) I_\lambda(x, s') ds' \end{aligned}$$

Introduction

Methodology

Results

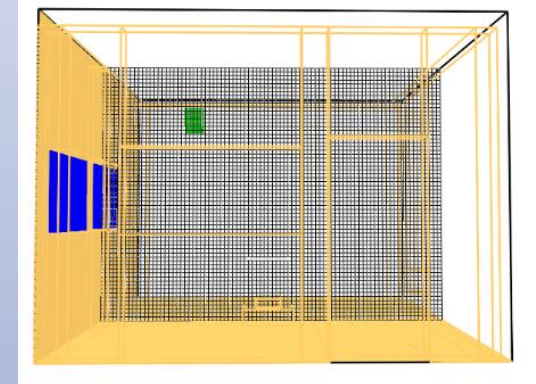
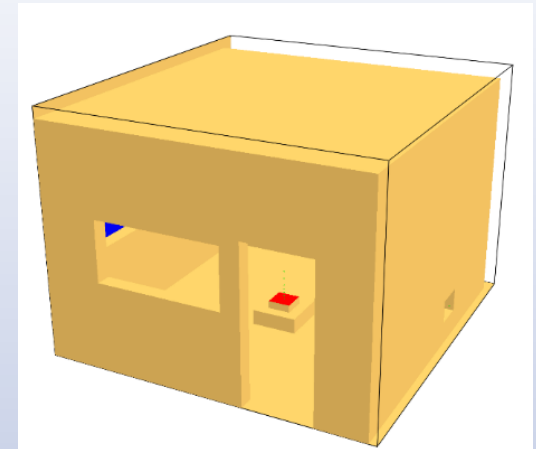
Conclusions

material	Conductivity (k) w/mk	Specific heat (c_p) j/kgk	Density (ρ) kg/m ³
Concrete	1.575	1000	2100
glass	1	750	2500
steel	50	450	7800
wood	0.13	1600	500

	Common Formula	Heat of combustion (ΔH_c) kj/kg	Soot yield kg/kg
Diesel	$C_{12}H_{23}$	42200	0.059

Nozzle 1	Nozzle 2
D=46 μ m	D=124.6 μ m
Operating pressure= 100bar	Operating pressure= 10bar
Flow rate= 11.9 l/min	Flow rate= 22.8 l/min
Velocity=10 m/s	Orifice diameter=0.0025m
Cone angle= 0-48°	Cone angle= 90
	K factor= 7.25

- Obstacle size: 25cm×25cm, 50cm×50cm, 1m×1m
- Obstacle thickness: 3mm
- Distance between floor and obstacle: 80cm and 1.5m



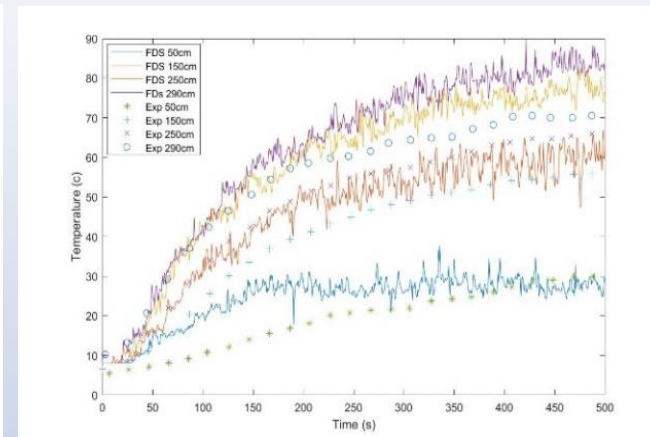
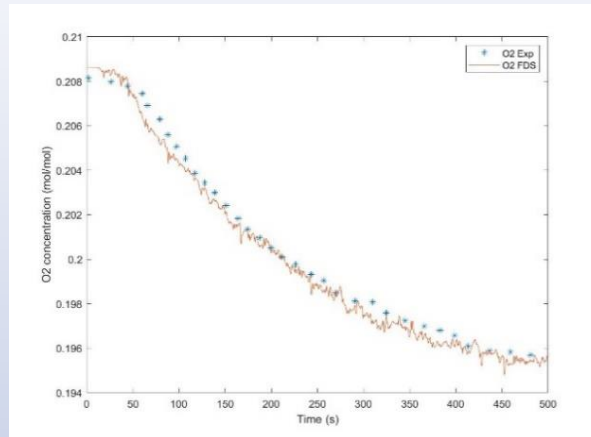
- Total number of 23 cases were defined and simulated
- A single mesh with around 500,000 cells was used
- HPC cluster was employed for simulations

Introduction

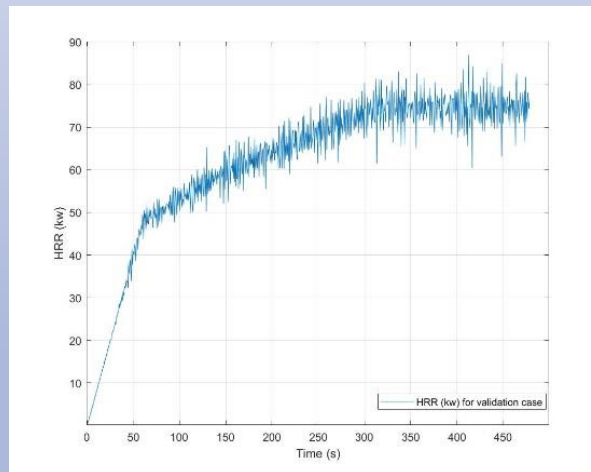
Methodology

Results

Conclusions



Data validation (Ref: A. Jenft, A. Collin, P. Boulet, G. Pianet, A. Breton, A. Muller, Experimental and numerical study of pool fire suppression using water mist, Fire Saf. J. 67 (2014))



HRR curve (peak value: 75kw)

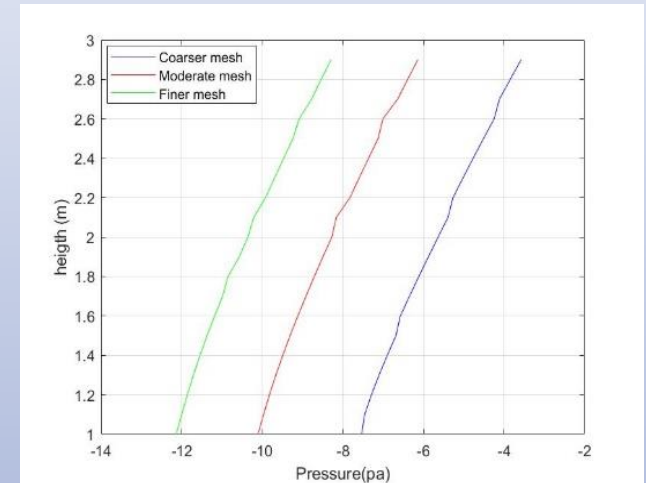
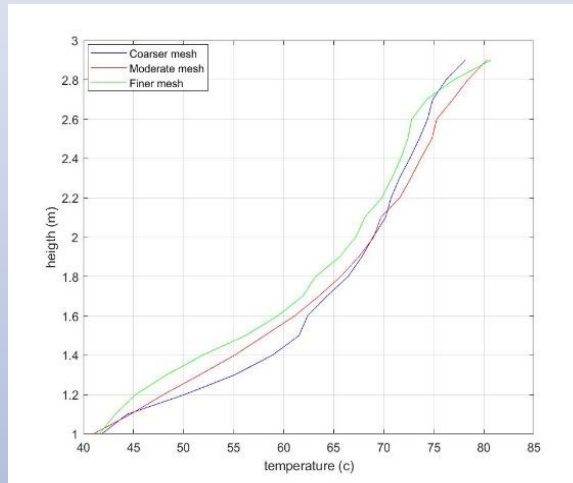
Introduction

Methodology

Results

Conclusions

$$D^* = \left(\frac{\dot{Q}}{\rho_\infty c_p T_\infty \sqrt{g}} \right)^{2/5} \longrightarrow D^* / \delta x$$



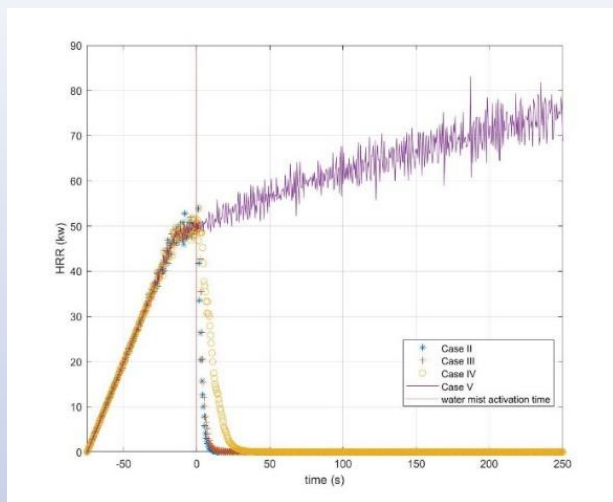
Coarse mesh
Moderate mesh
Fine mesh

Introduction

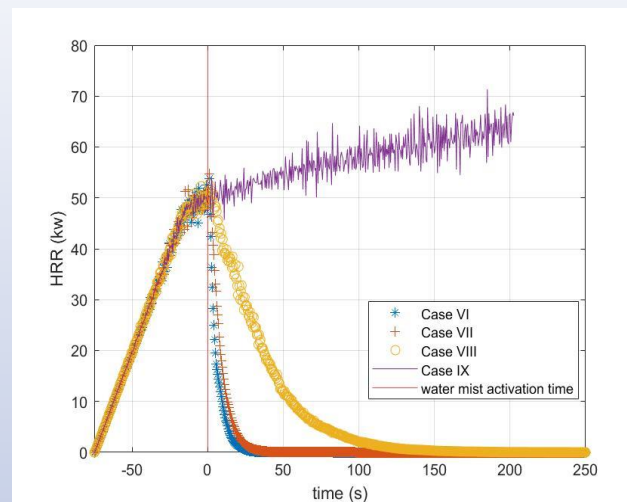
Methodology

Results

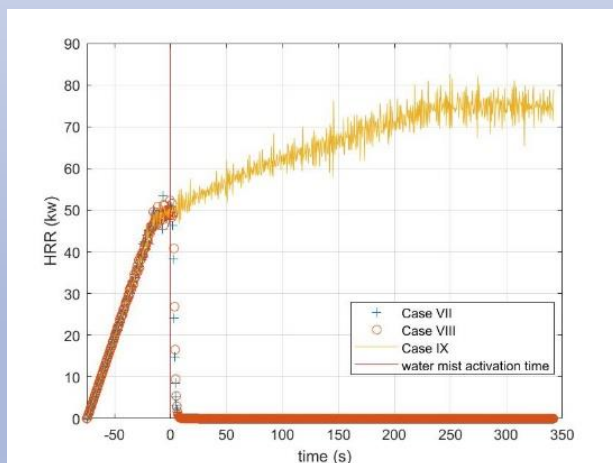
Conclusions



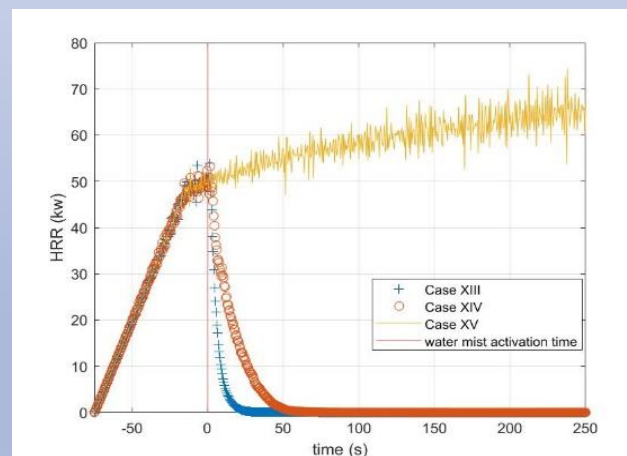
HRR evolution for cases II to V



HRR evolution for cases VI to IX



HRR evolution for cases X to XII



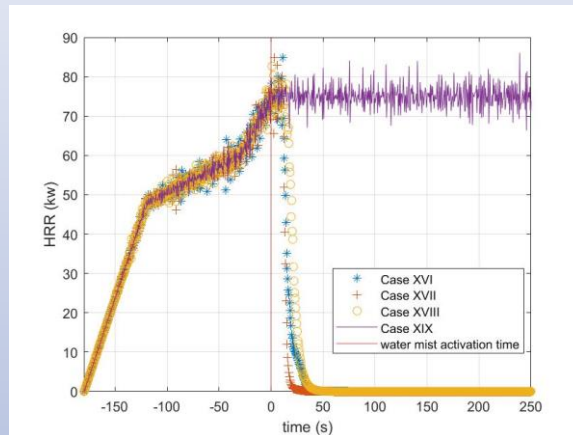
HRR evolution for cases XIII to XV

Introduction

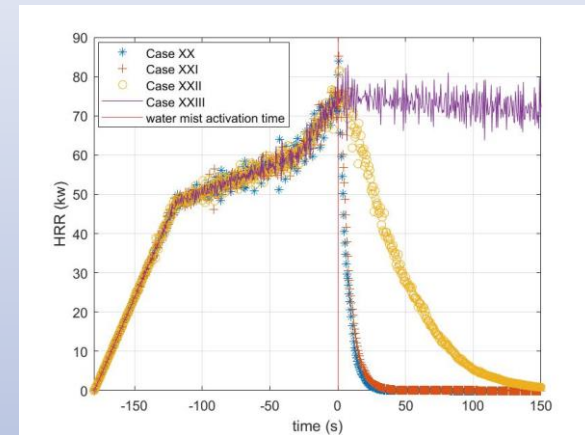
Methodology

Results

Conclusions



HRR evolution for cases XVI to XIX



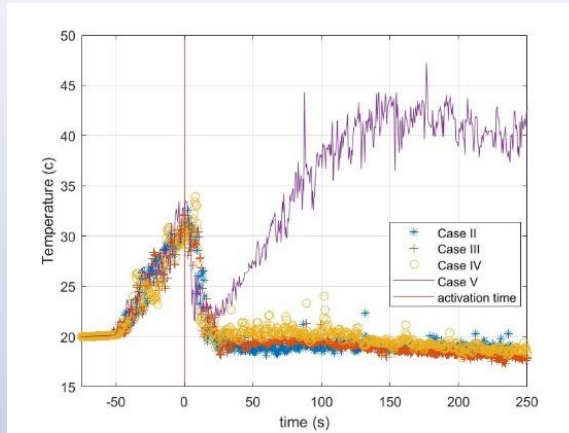
HRR evolution for cases XX to XXIII

Introduction

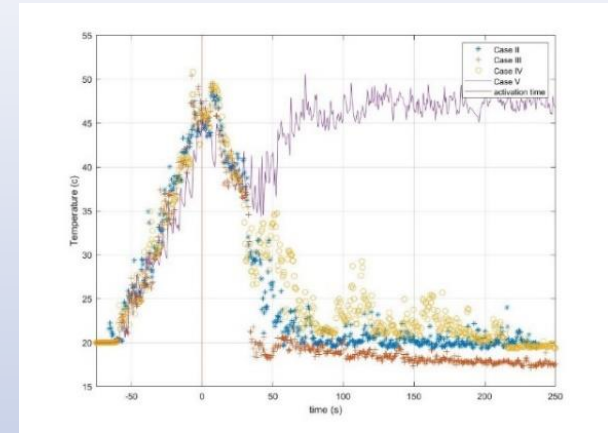
Methodology

Results

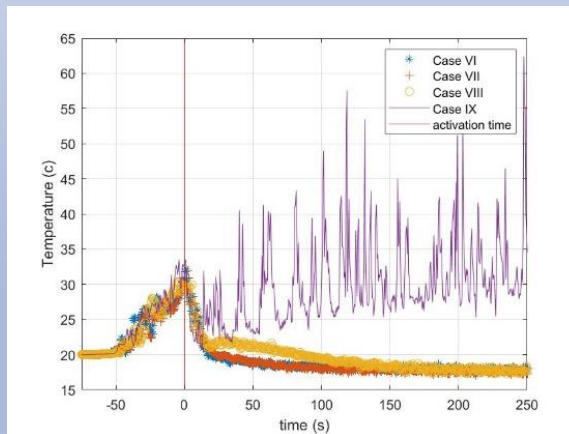
Conclusions



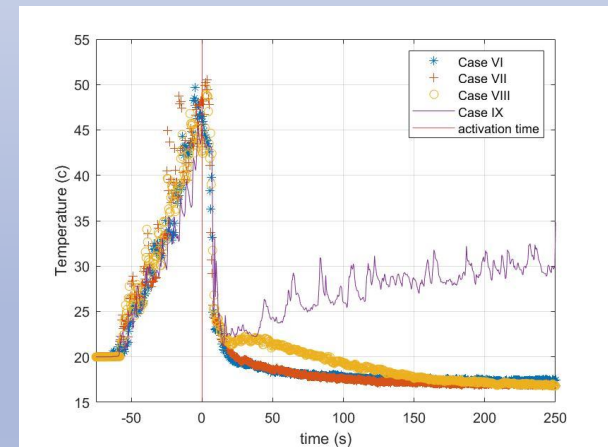
Temperature evolution on the corner
at the height 50cm for cases II to V



Temperature evolution on the corner
at the height 290cm for cases II to V



Temperature evolution on the corner at the
height 50cm for cases VI to IX



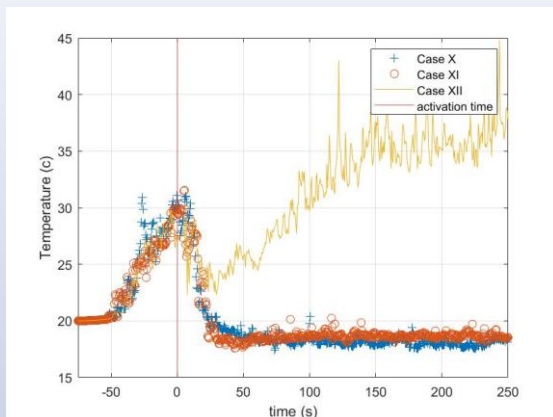
Temperature evolution on the corner at the
height 290cm for cases VI to IX

Introduction

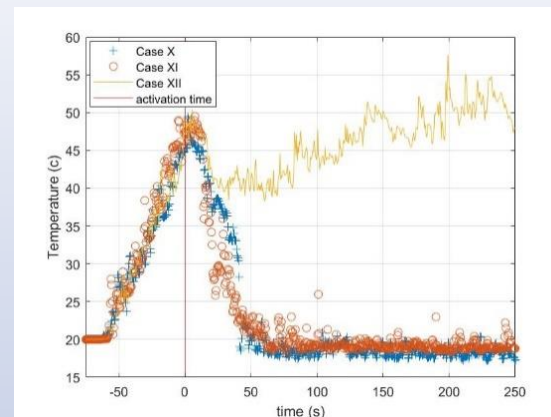
Methodology

Results

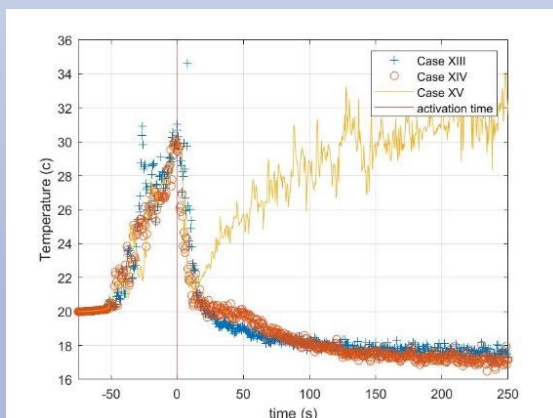
Conclusions



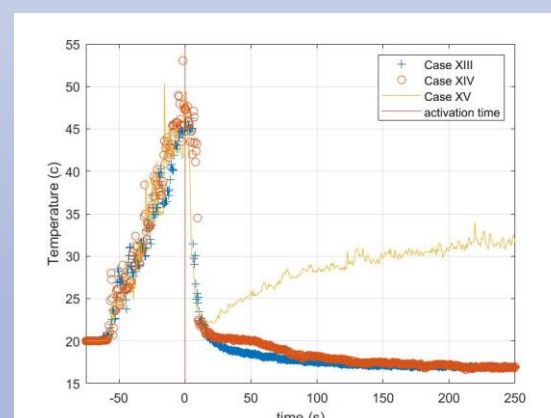
Temperature evolution on the corner at the height 50cm for cases X to XII



Temperature evolution on the corner at the height 290cm for cases X to XII



Temperature evolution on the corner at the height 50cm for cases XIII to XV



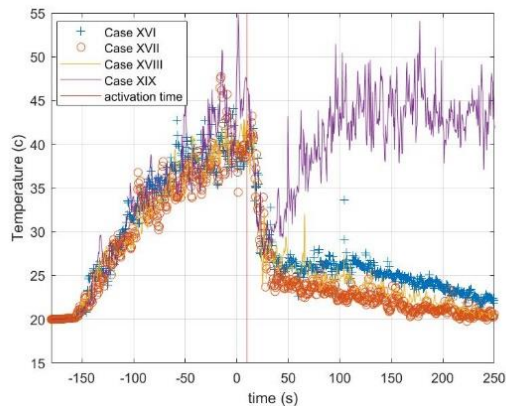
Temperature evolution on the corner at the height 290cm for cases XIII to XV

Introduction

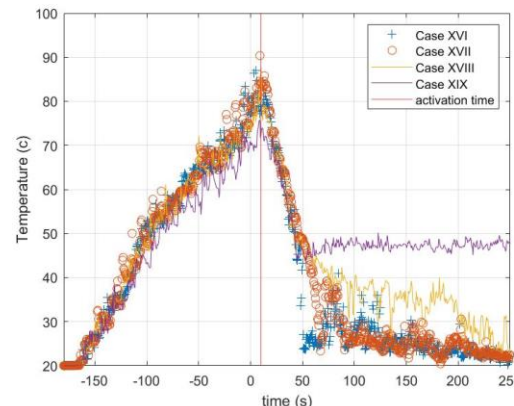
Methodology

Results

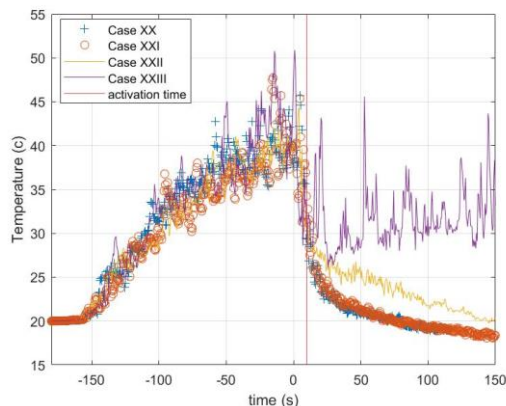
Conclusions



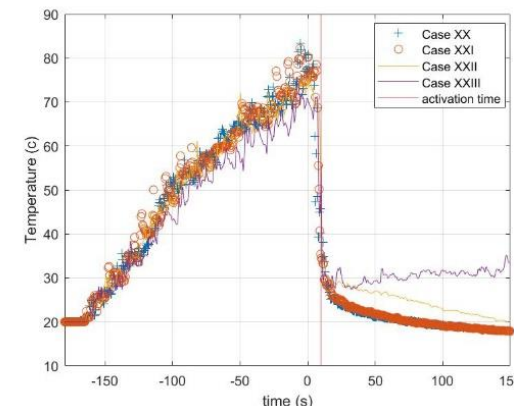
Temperature evolution on the corner at the height 50cm for cases XVI to XIX



Temperature evolution on the corner at the height 290cm for cases XVI to XIX



Temperature evolution on the corner at the height 50cm for cases XX to XXIII



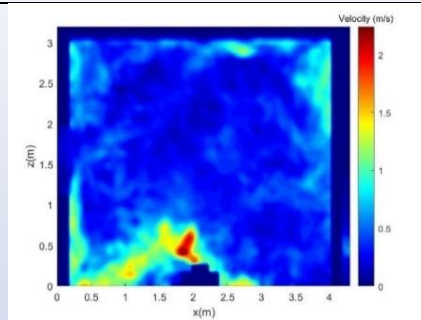
Temperature evolution on the corner at the height 290cm for cases XX to XXIII

Introduction

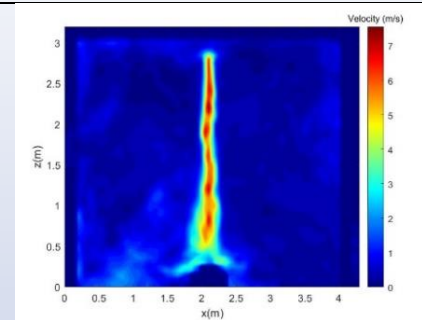
Methodology

Results

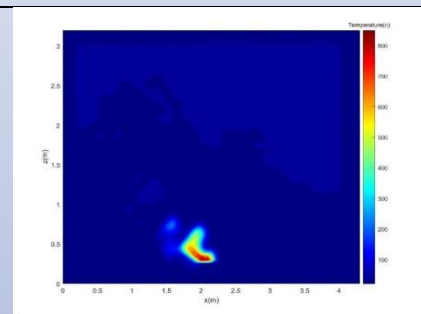
Conclusions



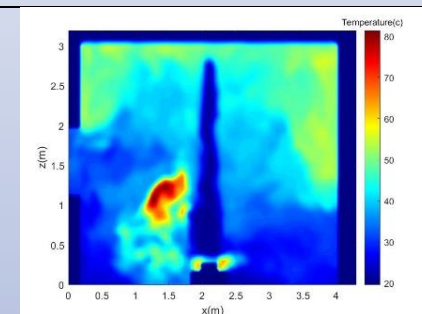
Velocity contour at 75s, just before the nozzle activation for case II



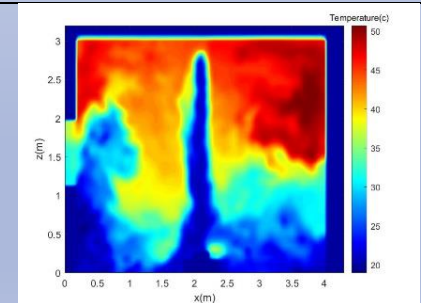
Velocity contour at 76s, just after the nozzle activation for case II



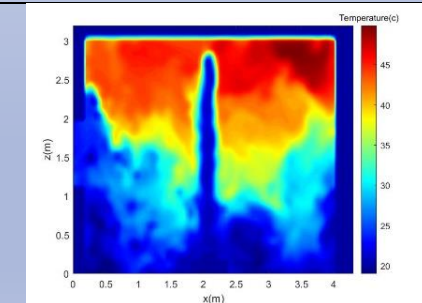
Temperature contour at 75s, just before the nozzle activation for case II



Temperature contour at 76s, just after the nozzle activation for case II



Temperature contour at 80s, 5s after the nozzle activation for case II



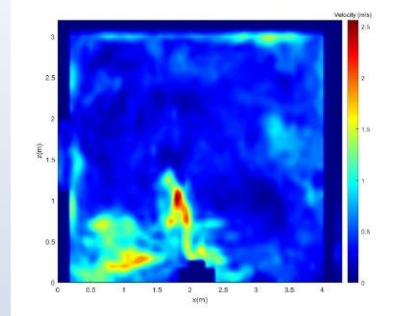
Temperature contour at 85s, 10s after the nozzle activation for case II

Introduction

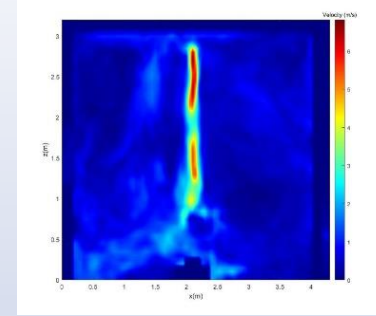
Methodology

Results

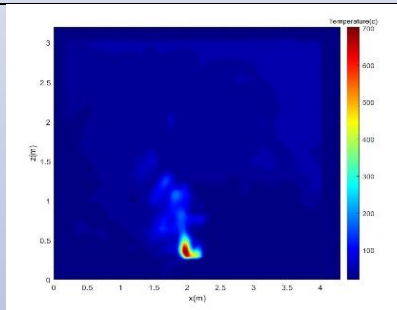
Conclusions



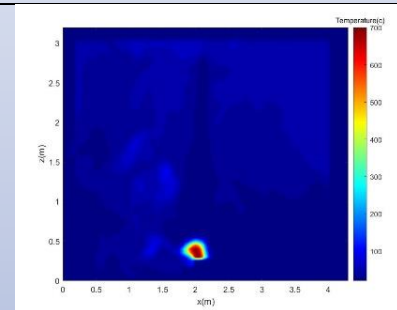
Velocity contour at 75s, just before the nozzle activation for case III



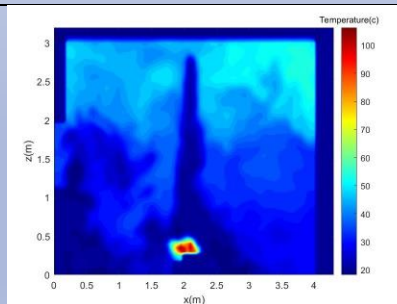
Velocity contour at 76s, just after the nozzle activation for case III



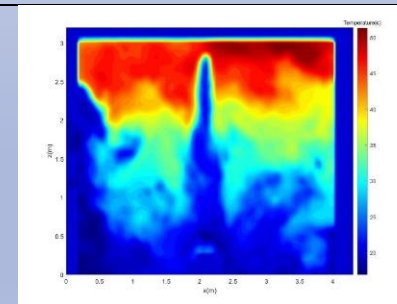
Temperature contour at 75s, just before the nozzle activation for case III



Temperature contour at 76s, just after the nozzle activation for case III



Temperature contour at 80s, 5s after the nozzle activation for case III



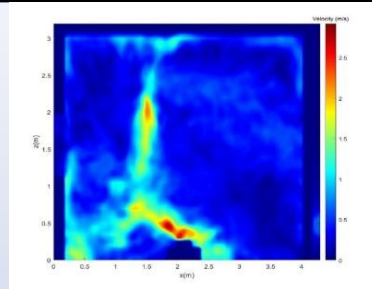
Temperature contour at 85s, 10s after the nozzle activation for case III

Introduction

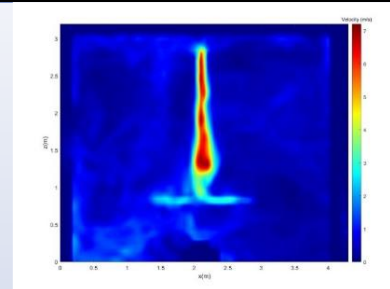
Methodology

Results

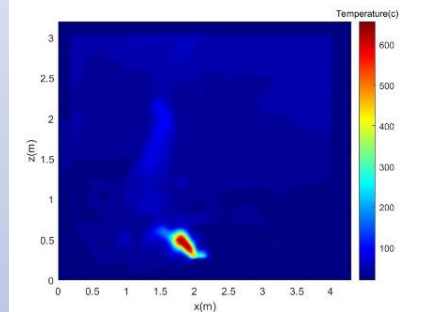
Conclusions



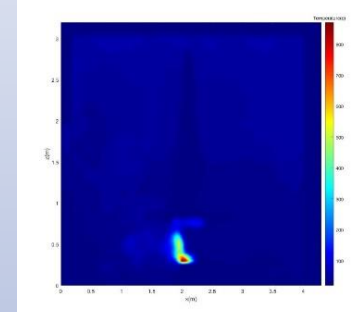
Velocity contour at 75s, just before the nozzle activation for case IV



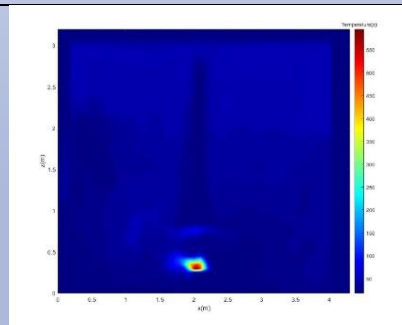
Velocity contour at 76s, just after the nozzle activation for case IV



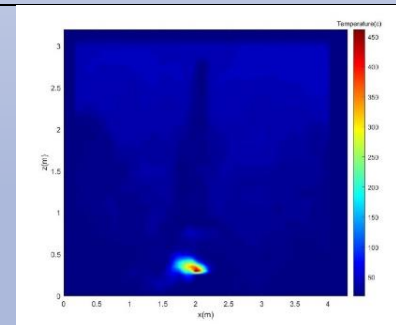
Temperature contour at 75s, just before the nozzle activation for case IV



Temperature contour at 76s, just after the nozzle activation for case IV



Temperature contour at 80s, 5s after the nozzle activation for case IV



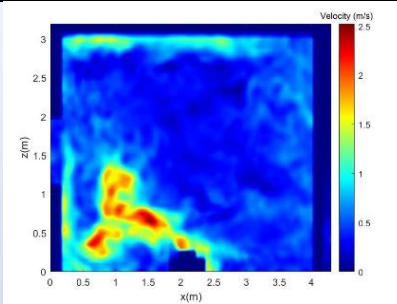
Temperature contour at 85s, 10s after the nozzle activation for case IV

Introduction

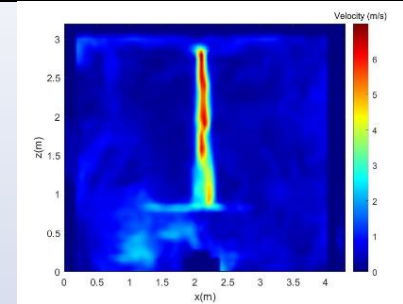
Methodology

Results

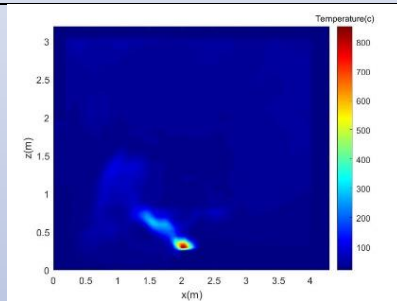
Conclusions



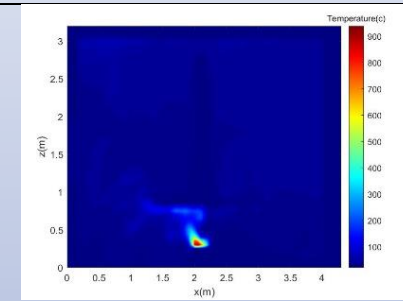
Velocity contour at 75s, just before the nozzle activation for case V



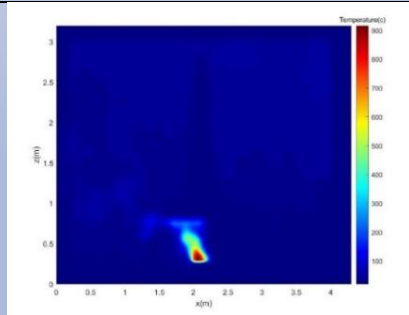
Velocity contour at 76s, just after the nozzle activation for case V



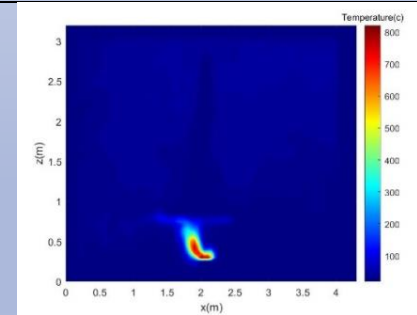
Temperature contour at 75s, just before the nozzle activation for case V



Temperature contour at 76s, just after the nozzle activation for case V



Temperature contour at 80s, 5s after the nozzle activation for case V



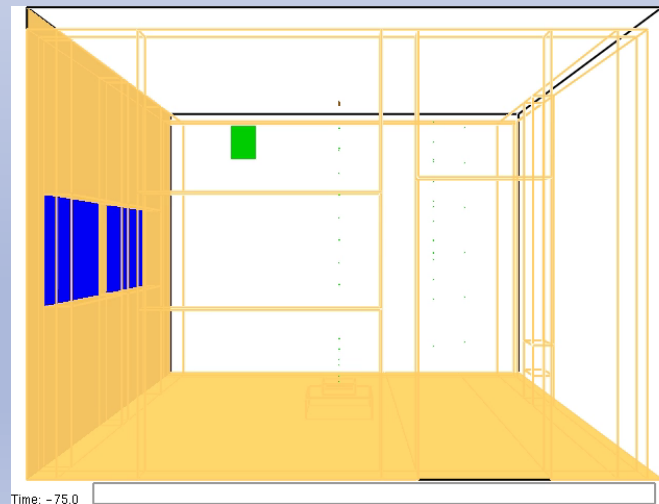
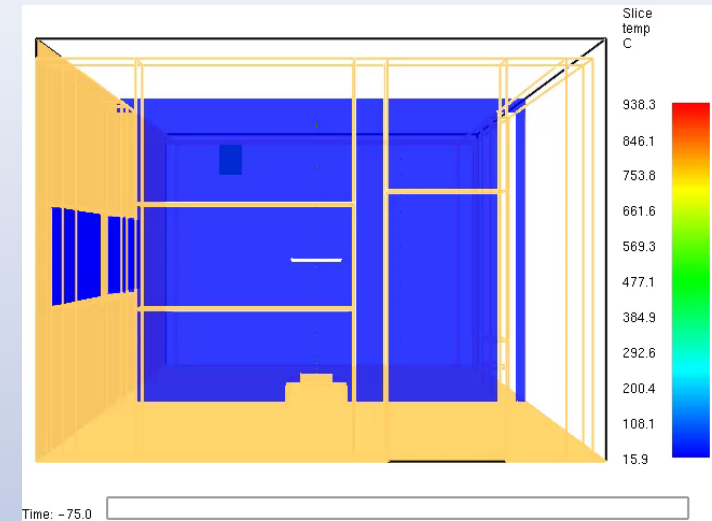
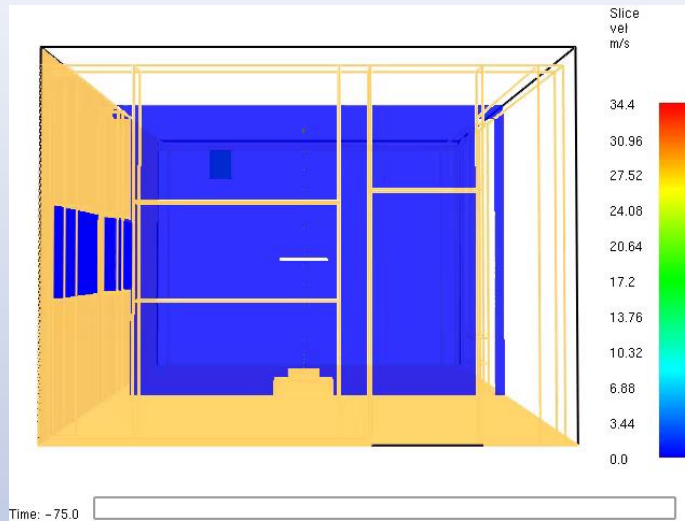
Temperature contour at 85s, 10s after the nozzle activation for case V

Introduction

Methodology

Results

Conclusions



Introduction

Methodology

Results

Conclusions

- The FDS models were successfully validated by the available experimental data.
- The grid independency study was carried out to find out the appropriate cell size with an acceptable accuracy.
- Both nozzles were able to suppress the fire with no obstacle at a very short time.
- Both nozzles failed to suppress the shielded fire when the obstacle size was 1m×1m above the fire.
- Nozzle 1 performed better compared to nozzle 2 in extinguishing the shielded fire when the obstacle sizes were 50cm×50cm and 25cm×25cm.
- In successful cases of extinguishment, the temperature inside the enclosure decreased sharply until reached to the atmosphere temperature.
- As there was no direct contact between the droplets and the fuel surface or the flames, the dominant fire extinguishing mechanisms were the oxygen displacement and the thermal radiation attenuation.
- Authors recommend doing more experiments and simulations on the performance of water mist systems and their capability to extinguish shielded fires

Let's work together!

Test facilities at Politecnico di Torino



- PDPA system for droplet size distribution measurement
- Enclosure fire facilities – thermocouple trees, gas analyzer, water mist system tests, HRR measurements, etc.



Thanks for your attention!

questions? comments?

Azad Hamzeshpour

PhD student

Energy Department - Politecnico di Torino

azad.hamzeshpour@polito.it

 Energy Center

Via Paolo Borsellino 38/16

10138 Torino, ITALY